Low-Cost Fiber Optic Cantilever Accelerometer With a Spherical Tip Based on Gaussian Beam Focusing

Lianjin Hong, Mingze Wu, Yongyao Chen, and Yue Li

***Abstract*—We propose and demonstrate a low-cost and simple fiber optic cantilever accelerometer with a spherical tip based on Gaussian beam focusing. The accelerometer consists of ceramic ferrule, ceramic sleeve, receiving fiber and emitting fiber, where both fibers are single mode fiber, the ferrule and sleeve have characteristics of high precision, which reduce the difficulty of optical alignment. The end of the emitting fiber is made into a spherical tip for focusing the Gaussian beam to improve sensitivity. When the accelerometer is in operation, the emitting fiber acts as a cantilever beam, the acceleration can be measured by detecting the transmission power. Further, our experimental results show that the spherical fiber tip can improve the acceleration sensitivity by 67% over 10 Hz–1000 Hz without reducing the working bandwidth. In addition, it is found that the fiber accelerometer has a high signal-to-noise ratio (SNR) up to 60 dB, and a low harmonic distortion of better than -30 dB, rendering a quasi-8-shaped directionality at the working frequency ranging from 10 Hz to 1200 Hz. This clever sensor structure may have potentials for developing high-performance and cost-effective accelerometers and hydrophones.**

***Index Terms*—Accelerometer, fiber optic cantilever, spherical tip, gaussian beam focusing, intensity demodulation.**

I. Introduction

ACCELEROMETERS play an important role in scientific research and various industrial fields such as robots, environmental surveillance, navigation systems and underwater acoustics [1]–[4]. Conventional accelerometers are mainly based on capacitive [5] and piezoelectric [6] techniques. These types of sensor have mature manufacturing technology, stable performance and commercialization. However, extremely vulnerable to electromagnetic interference is the key performance limitation of their application in harsh environments. To overcome the technical obstacle, the fiber-based acceleration sensing attracts considerable interests due to its electromagnetic interference immunity, light weight and high sensitivity.

Manuscript received June 3, 2021; revised July 17, 2021; accepted July 21, 2021. Date of publication July 26, 2021; date of current version August 6, 2021. This work was supported by the National Science and Technology Foundation of China under Grant 2018-JCJQ-ZQ-050. *(Corresponding author: Mingze Wu.)*

Lianjin Hong is with the Acoustic Science and Technology Laboratory, Harbin Engineering University, Harbin 150001, China, also with the Key Laboratory of Marine Information Acquisition and Security, Harbin Engineering University, Ministry of Industry and Information Technology, Harbin 150001, China, and also with the College of Underwater Acoustic Engineering, Harbin Engineering University, Harbin 150001, China (e-mail: honglianjin@hrbeu.edu.cn).

Mingze Wu, Yongyao Chen, and Yue Li are with the College of Underwater Acoustic Engineering, Harbin Engineering University, Harbin 150001, China (e-mail: wumingze@hrbeu.edu.cn; chenyongyao@hrbeu.edu.cn; liyue0987@hrbeu.edu.cn).

Digital Object Identifier 10.1109/JPHOT.2021.3099827

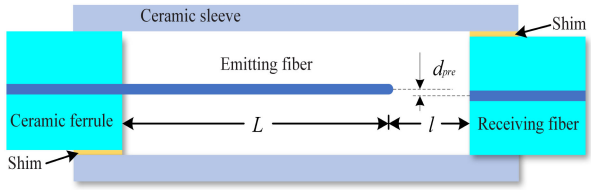

Fig. 1. Schematic diagram of the fiber cantilever accelerometer with a spherical tip.

In recent years, fiber optic cantilever beams have been widely studied in the field of vibration sensing. Wu *et al.* reported a fiber cantilever accelerometer based on modal interferometer with a large fringe visibility of up to 30 dB [7]. This accelerometer uses the lateral vibration of the fiber cantilever beam induced by vibrations to change the optical path difference between the cladding mode and the core mode. In the experiment, the accelerometer needs to set the initial operating point. This fiber cantilever sensor has a simple structure but complex operation. Guo *et al.* proposed a compact fiber cantilever ultrasonic sensor [8]. The sensor head is a Fabry-Perot interferometer formed by a single-mode fiber end face and a free end face of a fiber cantilever beam. The change of the F-P cavity length is caused by the axial vibration of the cantilever beam induced by ultrasonic and this sensor has a signal-to-noise ratio of up to 70 dB. However, the operating frequency of the fiber sensor is in the ultrasond band due to the limitation of the sensor structure. Dass *et al.* studied a high sensitivity fiber cantilever acoustic sensor based on direct light power measurement [9]. The sensor consists of a single mode fiber (SMF) micro tip and a SMF. The SMF micro tip place in front of a vertically cleaved SMF end face to receive the light emitted from the vertically cleaved SMF. The received power was modulated by the vibration of the SMF micro tip induced by acoustic. However, the packaging of this sensor is difficult because the rigorous alignment condition is difficult to achieve. Therefore, a vibration sensor with compact structure, low cost, high sensitivity and simple operation is desired.

In this paper, we proposed a fiber optic cantilever accelerometer with a spherical tip based on Gaussian beam focusing. The clever structural design enables it to have simple structure and low cost. It consists of a receiving fiber and an emitting fiber, which are encapsulated with ceramic ferrule and sleeve (Fig. 1). In the accelerometer, an emitting fiber acts as a cantilever beam responding to the acceleration, and its free end has a spherical tip to focus Gaussian Beam. The acceleration measurement is

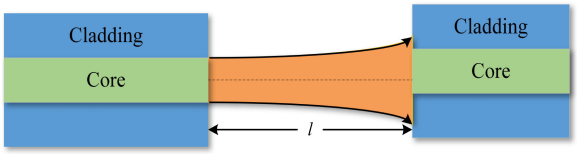

Fig. 2. Output light from the fiber with plane end face as a Gaussian beam.

obtained by using a low cost intensity modulation fiber-optic system. The experimental results show that the spherical tip can improve the sensitivity by 67% over 10 Hz–1000 Hz without reducing the working bandwidth. In addition, it is found that the fiber accelerometer has a high SNR up to 60 dB, and a low harmonic distortion of better than −30 dB, rendering a quasi-8-shaped directionality at the working frequency from 10 Hz to 1200 Hz.

II. Theory Analysis

The schematic diagram of the fiber cantilever accelerometer is shown in Fig. 1. It consists of a ceramic ferrule, a ceramic sleeve, and a pair of single mode receiving and emitting fibers. The emitting fiber acts as a cantilever beam mass-spring system.

The end of the emitting fiber is made into a sphere, with a gap l and an axial pre-offset d_{pre} between the fiber end and the receiving fiber. When a light beam is emitted from the fiber cantilever, part of the energy is received by the receiving fiber. The amount of received energy depends on the relative position of the fiber cantilever and receiving fiber. When there is acceleration, the cantilever is equivalent to a mass spring system, and the acceleration can be measured directly by detecting the power transmitting from the sensor. The deflection of the cantilever beam changes with the stimulus of the external acceleration, which leads to the change of the received intensity. Further, the deflection and slope of the free end of the fiber cantilever beam that subject to the external uniform load P could be given by the following equations [10]:

$$\delta_f = \frac{PL^4}{8EJ} \tag{1}$$

$$\theta_f = \frac{PL^3}{6EJ} \tag{2}$$

where P represent external force or pressure, E is the Young's modulus of the fiber, L is the length of the cantilever beam, J is the inertia moment. It is known that the intensity distribution of the fundamental mode of a single mode fiber can be approximated by a Gaussian field distribution [11]–[13]. When the end face of the emitting fiber is a flat plane shown in Fig. 2, the intensity distribution in the cross section at the free end can be expressed as [14]

$$I_r = I_0 exp\left(\frac{-2r^2}{w_0^2}\right) \tag{3}$$

where I_r is the light intensity at a fiber radius of r, I_0 is the light intensity at $r = 0$, w_0 is the mode-field radius of fiber.

Further, according to the characteristics of Gaussian beam, the intensity distribution of the light beam in the air cavity (the air gap region between emitting and receiving fibers) can be expressed as

$$I(r,z) = I_0' exp\left(-\frac{2r^2}{w^2(z)}\right) \tag{4}$$

where $I_0' = I_0(w_0/w(z))^2$, $w(z) = w_0[1 + (\theta_0 z/w_0)^2]^{1/2}$ is the mode-field radius, θ_0 is the divergence angle of a Gaussian beam that is given by $\theta_0 = w_0/z_0 = \lambda/\pi w_0 = \sin^{-1} NA$, NA is the numerical aperture of the fiber, z_0 is called Rayleigh distance and z represents the distance from a point in the air cavity to the end face of the cantilever. The mode-field radius of a single mode fiber w_0 can be obtained by the Matthews criterion [14]. We can see from (4) that $I_r = I(r, 0)$. The corresponding power received by the receiving fiber can be calculated by taking the integral of the light field distribution over the receiving fiber core

$$W = \iint_S I(r,l) r dr d\theta = \iint_S I_0' exp\left(-\frac{2r^2}{w^2(l)}\right) r dr d\theta \tag{5}$$

where S is the area of the receiving fiber core. Noted that, the received energy could be modulated by the axis offset of the two fibers. The calculated received power by (5) is plotted as a function of the axis offset d shown in Fig. 3(a) for air gap lengths l of 20 μm, 40 μm, 60 μm, 80 μm and 100 μm, respectively.

It can be seen from the Fig. 3(a) that when there is no axis offset, the received energy is the maximum. As the amount of axis offset increases, the received energy gradually decreases. Near the $d = 0$, the energy changes slowly, and then with the increase of d, the rate of energy reduction gradually accelerates and stabilizes at a constant value for a certain distance which is the linear region. In the production of the accelerometers, d_{pre} should be set in this linear region. When the offset increases to a certain value, the change of received energy slows down again, and the energy gradually approaches zero. The curves with different l have the same changing trend (see Fig. 3(a)). As l increases, the rate of energy reduction will decrease. This is because the Gaussian beam broadens as the propagation distance increases. In summary, on the end face of the receiving fiber, the smaller the mode-field radius of the Gaussian beam is, the higher the sensitivity of the accelerometer can be obtained. For this type of accelerometer, the pre-offset d_{pre} should be in the linear region, the slope of linear region in Fig. 3(a) reflects the sensitivity of the sensor. According to the numerical results, when d_{pre} is in the linear region we can express the change of received power as following.

$$\Delta W = I_0' \cdot k_l \cdot \Delta d \tag{6}$$

where k_l is a constant varying with l. According to the geometric relation in Fig. 4, Δd can be further expressed as following

$$d = d_{pre} + \delta_f + l \cdot \theta_f = d_{pre} + \frac{PL^4}{8EJ} + \frac{PL^3 l}{6EJ} \tag{7}$$

$$\Delta d = \Delta\delta_f + l \cdot \Delta\theta_f = \frac{\Delta PL^4}{8EJ} + \frac{\Delta PL^3 l}{6EJ}, \tag{8}$$

providing that a small deflection angle of the cantilever is applied here.

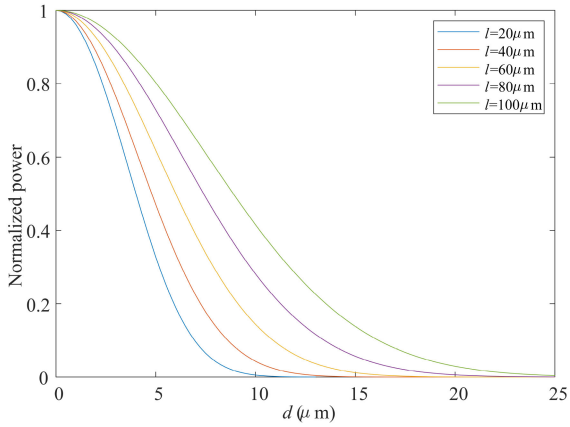

(a)

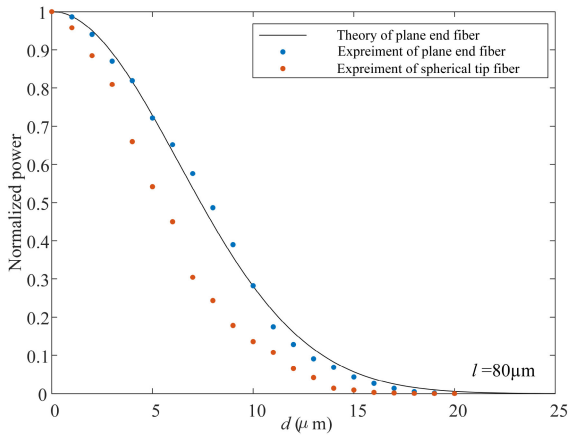

(b)

Fig. 3. (Color online) (a) The calculated received power curves. (b) The experimental receiving power curve of the fiber with a spherical tip measured at $l = 80$ m, in comparison with the experimental and theoretical power distribution of the fiber with a plane end face.

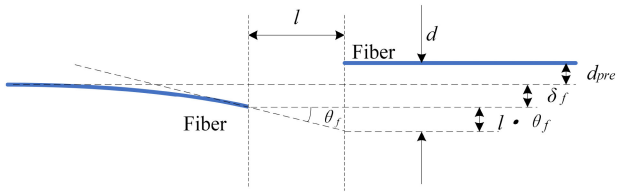

Fig. 4. The geometric relation of the emitting fiber and receiving fiber with a small deflection angle.

The pressure responsivity can be transformed to the acceleration responsivity by using [15]

$$\Delta P = \frac{\pi}{2} r' \rho \Delta a \tag{9}$$

which gives the acceleration responsivity of

$$\begin{aligned} \frac{\Delta W}{\Delta a} &= \frac{\pi}{2} r' I_0' \rho k_l \left(\frac{L^4}{8EJ} + \frac{L^3 l}{6EJ} \right) \\ &= \frac{\pi}{2} r' I_0' \rho k_l \frac{L^3}{2EJ} \left(\frac{L}{4} + \frac{l}{3} \right) \end{aligned} \tag{10}$$

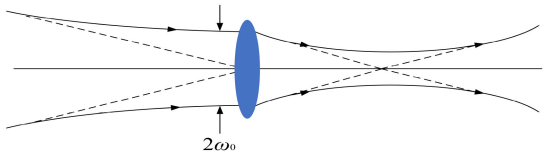

Fig. 5. Focusing a gaussian beam with a lens at the beam waist.

where ρ is the fiber density, a is acceleration and r' is the radius of fiber. The value of l is small relative to the value of L, so the term containing l in (10) can be ignored. The acceleration sensitivity in units of g^{-1} can be expressed as

$$\frac{\Delta W}{\Delta a} \approx (9.8) \frac{\pi}{2} r' I_0' \rho k_l \frac{L^4}{8EJ} \tag{11}$$

From the above equation, it is obvious that, the acceleration sensitivity is affected by the parameters of L and k_l. It should be pointed out that, increasing the length L can improve the sensitivity, but the value of L determines the resonant frequency of the cantilever which limits the effective working bandwidth of the sensor. The first-order natural frequency (f_0) of the fiber optics cantilever is defined as

$$f_0 = \frac{3.516}{2\pi L^2} \sqrt{\frac{EJ}{\rho A_S}} \tag{12}$$

where ρ is the density of the fiber, A_S is the cross-sectional area of the fiber. The accelerometer should have a flat response within the operating frequency. The maximum operating frequency should be less than the resonant frequency. Therefore, the selection of the value of L is limited to the compromise between sensitivity and the operating frequency. Another way to increase sensitivity is to increase the value of k_l. This requires reducing the radius of the mode field on the end face of the receiving fiber. Therefore, in order to improve the sensitivity, a spherical tip fiber structure is proposed to achieve focused Gaussian beam to reduce the mode field size, which could act as a thin lens to improve the sensitivity without sacrificing the rang of working bandwidth (Fig. 5). Noted that, the spherical tip can be made by optical fiber fusion splicer, and the optical microscope image of the fiber spherical tip is shown in Fig. 6(a). To verify the focusing effect of the spherical tip, the receiving fiber and the emitting fiber with a spherical tip were fixed on two five-dimensional fiber alignment brackets for testing. The distance between the two fibers is set to 80 μm. As a comparison, an emitting fiber with a plane end face is also tested under the same conditions. The test result is shown in Fig. 3(b), the experimental received power of the emitting fiber with plane end agree with the simulation results of (5), which proves the correctness of the above theory model. The experimental result of emitting fiber with a spherical tip illustrates that the received power decreases faster as the amount of offset increases, which indicates the Gaussian beam has been focused. Furthermore, we introduce a coefficient k_s to express the gain due to the beam focusing and the acceleration sensitivity can be expressed as

$$\frac{\Delta W}{\Delta a} \approx (9.8) \frac{\pi}{2} r' I_0' \rho k_l k_s \frac{L^4}{8EJ} \tag{13}$$

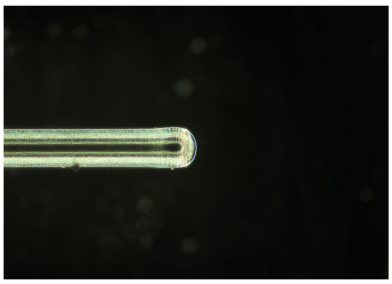

(a)

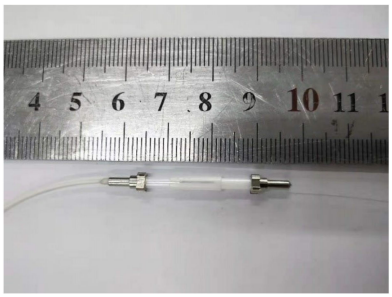

(b)

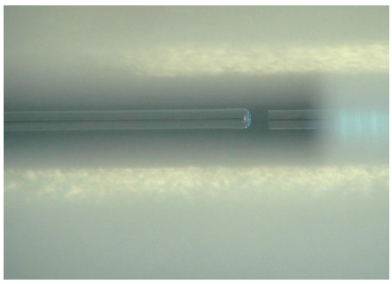

(c)

Fig. 6. (a) The optical microscope image of the fiber spherical tip; (b) The assembled fiber accelerometer; (c) The micrograph of the internal structure of the sensor.

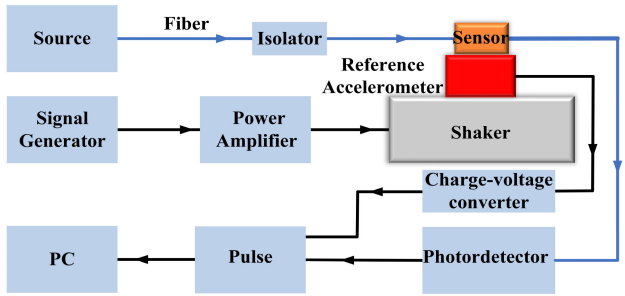

Fig. 7. Arrangement of the experimental system.

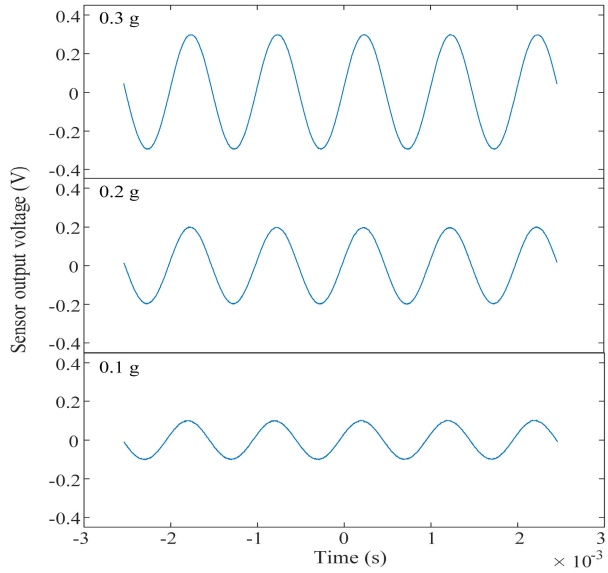

Fig. 8. The time domain spectra of the fiber spherical tip accelerometer by the drive acceleration of 0.1 g, 0.2 g and 0.3 g at a sinusoidal signal of 1000 Hz.

According to the analysis and the test result, the value of k_s is greater than one, so the higher sensitivity can be obtained.

III. Experiment

The ceramic ferrule and ceramic sleeve are selected for sensor fabrication. The sensor head is shown in Fig. 6(b). The ceramic sleeve has a gap that enables the measurement of parameters l and d_{pre} during the manufacturing process of the sensor. The emitting and receiving fibers pass through a ceramic ferrule. The length of the cantilever beam is selected according to the actual application and fixed with ultraviolet (UV) curing adhesive. The receiving fiber end is exposed a short distance from ceramic ferrule for accurately measure l such as in Fig. 6(c). The two ferrules are connected by a ceramic sleeve. The pre-offset d_{pre} can be achieved by embedding a shim of a certain thickness between the ferrule and the sleeve, as shown in Fig. 1.

The experimental system is shown in the Fig. 7, which is composed of SLD source (THORLABS), isolator, photodetector with a gain of 25 dB, signal generator (Agilent 33522 A), power amplifier (B & K 2719), shaker (B & K 4809), charge-voltage converter (B & K 2647), pulse (B & K 3109) and a reference accelerometer (B & K 8305). A fiber cantilever accelerometer with a spherical tip was fabricated with $d_{pre} = 10\,\mu$m, $l = 100\,\mu$m and $L = 7.1$ mm. The accelerometer is measured with the experimental system, whose time-domain spectra of the fiber cantilever sensor for acceleration 0.1 g, 0.2 g and 0.3 g at the sinusoidal frequency of 1000 Hz is shown in Fig. 8, respectively. The relationship between the output voltage and the time is consistent with the sinusoidal signal. The corresponding peak-to-peak output voltages are 0.201 V, 0.403 V, and 0.601 V, respectively, which has a good linear relationship with acceleration. We also tested the sensor continuously within 1 h under the same excitation condition at a reference frequency of 1000 Hz. The deviation of the sensor output voltage is within $\pm 0.76\%$. From the test, it is confirmed that this accelerometer has a good stability. The frequency response of the sensor is shown in Fig. 9. The resonant frequency of the fiber cantilever with a spherical tip is 2286 Hz. The frequency response is almost constant in the range of 10 Hz–1200 Hz which corresponds to the linear working range of the accelerometer. Fig. 10 shows the relative power spectrum of the accelerometer with an acceleration of 0.3 g at 1000 Hz. It shows that the relative signal at 1000 Hz is

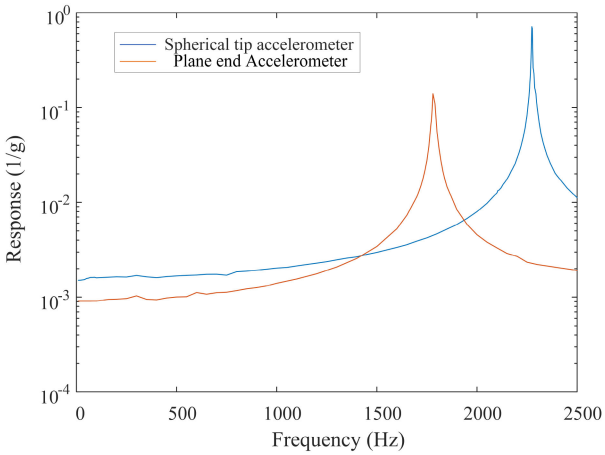

Fig. 9. (Color online) Measured frequency response of two fiber optical accelerometers.

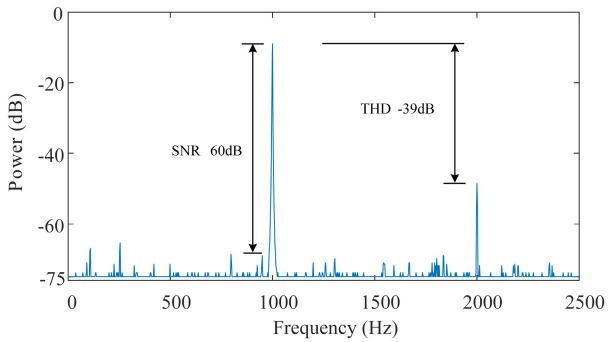

Fig. 10. Frequency domain response of the sensor driven by 0.3 g, 1000 Hz.

very strong. In addition, it is found that, the harmonic distortion is -39 dB which means that the sensor response is linear [16], and a high signal-to-noise ratio (SNR) up to about 60 dB can be obtained from the Fig. 10.

For comparison, the fiber cantilever with a plane end face was fabricated with similar geometric parameters ($d_{pre} = 10$ m, $l = 100$ m and $L = 7.3$ mm). The normalized sensitivity curves of the two sensors (the plane fiber end and spherical fiber end) ranging from 10 Hz to 2500 Hz are shown in Fig. 9. The resonance frequency of the accelerometer with a plane fiber end is 1780 Hz which is different from the resonance frequency of the accelerometer with a spherical tip. This could be due to the difference enface structures and slight differences between the lengths of the cantilevers. Fig. 9 shows that the spherical tip of fiber cantilever can improve the sensitivity of the sensor without reducing the working bandwidth and the sensitivity was improved by 67% over 10 Hz–1000 Hz.

Furthermore, it is found that the fiber accelerometer has directivity which is due to axisymmetric energy distribution of the Gaussian beam. Due to the fact that the change of received power is caused by the vibration-induced variation of the energy distribution on the end face of receiving fiber. The energy distribution on the end face of the receiving fiber is symmetrical about the axis whose direction is along the pre-offset. Due to

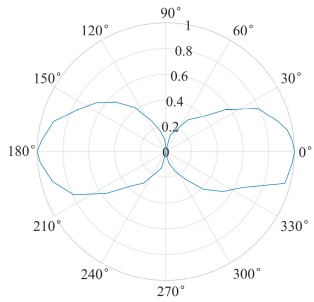

Fig. 11. The directional response of the fiber optical accelerometer with a spherical tip.

the pre-offset setting, the energy distribution changes linearly along the pre-offset direction. Above measurements were made with the sensor being driven along the direction of pre-offset which is its most responsive axis. When the vibration is along the direction perpendicular to the pre-offset, the variation of received energy is slight because of the bilateral symmetry of the energy distribution about the pre-offset on the end face of the receiving fiber. This is equivalent to not setting a pre-offset in the direction of perpendicular to the pre-offset. As can be seen from Fig. 3(a), the slopes of the curves are almost 0 at $d_{pre} = 0$, therefore the sensor is insensitive in this direction. The proposed fiber cantilever accelerometer with a spherical tip is investigated by applying acceleration in different directions. For example, the normalized directional response at 1000 Hz is shown in Fig. 11 and the sensor has a quasi-8-shaped directionality.

IV. Conclusion and Discussion

In this paper, we demonstrated a fiber spherical tip accelerometer. The fiber accelerometer consists of ceramic ferrule, ceramic sleeve, receiving fiber and emitting fiber. The ceramic ferrule and the ceramic sleeve are commercial standard parts with extremely high precision, which reduces the difficulty of optical alignment, while at very low cost. The end of the emitting optical fiber is made into a spherical tip by arc discharge to focus Gaussian Beam. Simple analytical models have been derived to calculate the received power, and the analytical results were in good agreement with the measured results. A prototype fiber accelerometer of the spherical tip sensor was fabricated and calibrated in the experiments. The resonant frequency of the prototype is 2286 Hz, which is determined by the length of the cantilever beam. The working range of the prototype is 10 Hz–1200 Hz. For comparison, a plane end face fiber accelerometer was fabricated, and the measurements of sensitivity of the two sensors (with and without the spherical tips) demonstrate that the spherical tip sensor can improve the sensitivity by over 67% ranging from 10 Hz–1000 Hz without reducing the working bandwidth. Further, the prototype sensor shows a high SNR up to about 60 dB, a high harmonic distortion of -39 dB, and a quasi-8-shaped directionality. The proposed fiber accelerometer has advantages of good sensitivity, simple structure, convenient manufacture and low cost. According to previous reports [17], [18], this type of sensor can be improved for vibration displacement or vibration velocity sensing by changing the fluid viscous

damping around the cantilever beam, which could be attractive for vector hydrophones and has great potential for many sensing applications.

REFERENCES

[1] Q. Xueguang, S. Zhihua, B. Weijia and R. Qiangzhou, "Fiber Bragg grating sensors for the oil industry," *Sensors*, vol. 17, no. 3, Feb. 2017.

[2] P. Ullah, V. Ragot, P. Zwahlen, and F. Rudolf. ,"A new high performance sigma-delta mems accelerometer for inertial navigation," in *Proc. DGON Inert. Sensors Syst.*, Oct. 2015, pp. 1-13. [Online]. Available: https://ieeexplore.ieee.org/document/7314257

[3] M. S. Mahmood, Z. Celik-butler, and D. P. Butler. , "Wafer-level packaged flexible and bendable mems accelerometer for robotics and prosthetics," in *Proc. SAS - IEEE Sens. Appl. Symp.*, Apr. 2017, pp. 1-5. [Online]. Available: https://ieeexplore.ieee.org/document/7894033

[4] C. Peng, X. Zhang, and Z. Meng, "Bearing estimation for optical fiber vector hydrophone with in-band resonance," *Appl. Acoust.*, vol. 158, no. 107055, pp. 1–7, Jan. 2020.

[5] A. Beliveau, G. T. Spencer, K. A. Thomas, and S. L. Roberson, "Evaluation of mems capacitive accelerometers," *IEEE Des. Test. Comput.*, vol. 16, no. 4, pp. 48–56, Oct. 1999.

[6] S. Tadigadapa and K. Mateti, "Piezoelectric mems sensors: State-of-the-art and perspectives," *Meas. Sci. Technol.*, vol. 20, no. 9, Jul. 2009.

[7] X. Wu, X. Wang, S. Li, and S. Huang, "Cantilever fiber-optic accelerometer based on modal interferometer," *IEEE Photon. Technol. Lett.*, vol. 27, no. 15, pp. 1632–1635, Aug. 2015.

[8] T. Guo, P. Li, T. Zhang, and X. Qiao, "Compact fiber-optic ultrasonic sensor using an encapsulated micro-cantilever interferometer," *Appl. Opt.*, vol. 58, no. 13. pp. 3331–3337, Apr. 2019.

[9] S. Dass, S. Halder, J. Sharma, R. Jha, "Fiber cantilever based acoustic sensor," in *Proc. Opt. InfoBase Conf. Pap.*, Sep. 2017, pp. JW4A-67. [Online]. Available: https://www.osapublishing.org/abstract.cfm?URI=FiO-2017-JW4A.67

[10] J. M. Gere and B. J. Goodno, *Mechanics of Materials*. 9th ed., Boston, Massachusetts, USA: Cengage Learning, 2018, pp. 822–823.

[11] M. Taghavi, H. Latifi, G. M. Parsanasab, A. Abedi, H. Nikbakht, and M. J. Sharifi, "Simulation, fabrication, and characterization of a sensitive SU-8-based Fabry-Pérot MOEMS accelerometer," *J. Lightw. Technol.*, vol. 37, no. 9, pp. 1893–1902, May 2019.

[12] L. Su and S. R. Elliott, "All-fiber microcantilever sensor monitored by a low-cost fiber-to-tip structure with subnanometer resolution," *Opt. Lett.*, vol. 35, no. 8, pp. 1212–1214, Apr. 2010.

[13] V. Trudel and Y. St-amant, "One-dimensional single-mode fiber-optic displacement sensors for submillimeter measurements," *Appl. Opt.*, vol. 48, no. 26. pp. 4851–4857, Sep. 2009.

[14] D. Marcuse, "Loss analysis of single-mode fiber splices," *Bell System Tech. J.*, vol. 56, no. 5, pp. 703–718, Jun. 1977.

[15] G. A. Cranch and P. J. Nash, "High-responsivity fiber-optic flexural disk accelerometers," *J. Lightw. Technol.*, vol. 18, no. 9, pp. 1233–1243. Sep. 2000.

[16] O. Kilic, M. Digonnet, G. S. Kino, and O. Solgaard, "Miniature photonic-crystal hydrophone optimized for ocean acoustics," *J. Acoust. Soc. Amer.*, vol. 129, no. 4, pp. 1837–1850, Apr. 2011.

[17] J. E. Sader, "Frequency response of cantilever beams immersed in viscous fluids with applications to the atomic force microscope," *J. Appl. Phys.*, vol. 84, no. 1, pp. 64–76, Jul. 1998.

[18] G. A. Cranch, G. A. Miller, and C. K. Kirkendall, "Fiber-optic, cantilever-type acoustic motion velocity hydrophone," *J. Acoust. Soc. Amer.*, vol. 132, no. 1, pp. 03–114, Jul. 2012.